INTERNATIONAL JOURNAL FOR NUMERICAL METHODS IN FLUIDS, VOL. 18, 107–122 (1994)

AN EFFICIENT SHOCK-CAPTURING ALGORITHM FOR COMPRESSIBLE FLOWS IN A DUCT OF VARIABLE CROSS-SECTION

P. GLAISTER

Department of Mathematics, PO Box 220, University of Reading, Reading RG6 2AX, U.K.

SUMMARY

A numerical scheme is presented for the solution of the Euler equations of compressible flow of a gas in a single spatial co-ordinate. This includes flow in a duct of variable cross-section as well as flow with slab, cylindrical or spherical symmetry and can prove useful when testing codes for the two-dimensional equations governing compressible flow of a gas. The resulting scheme requires an average of the flow variables across the interface between cells and for computational efficiency this average is chosen to be the arithmetic mean, which is in contrast to the usual 'square root' averages found in this type of scheme. The scheme is applied with success to five problems with either slab or cylindrical symmetry and a comparison is made in the cylindrical case with results from a two-dimensional problem with no sources.

KEY WORDS Euler equations Flux difference splitting Duct flow

1. INTRODUCTION

The approximate Riemann solver of Roe[1] has proved successful in its application to a number of problems in unsteady gas dynamics. Other Riemann solvers developed along different lines have also been equally successful in this area of CFD (see e.g. Reference 2). The pioneering work of Roe has also been extended in other areas such as MHD, but some of the original conditions for constructing the Jacobian matrix have to be abandoned sometimes (see e.g. Reference 3).

Recently[4] an approximate Riemann solver of the Roe type was developed for the shallow water equations which used the arithmetic mean for the average of the flow variables across a cell interface. The purpose of this paper is to present a similar type of Riemann solver for the Euler equations for a duct of variable cross-section and using the arithmetic mean for computational efficiency. This is in contrast to the usual 'square root' averaging of Roe's Riemann solver. As well as the usual case of slab symmetry, this includes flows with cylindrical or spherical symmetry. The scheme is applied to five problems with interacting and/or reflecting shocks in slab or cylindrical geometry. The arithmetic mean has also been used for the steady Euler equation scheme of Dick[5] where the equations and underlying Jacobian structure are different from those of this paper.

2. EQUATIONS OF FLOW

The 'one-dimensional' equations governing compressible flow of a gas can be written as

0271–2091/94/010107–16$13.00

Received May 1993
Revised September 1993

$$\rho_t + \frac{1}{S(r)}(S(r)\rho u)_r = 0, \tag{1a}$$

$$(\rho u)_t + \frac{1}{S(r)}(S(r)\rho u^2)_r = -p_r, \tag{1b}$$

$$e_t + \frac{1}{S(r)}(S(r)u(e+p))_r = 0, \tag{1c}$$

where the total energy

$$e = \frac{p}{\gamma - 1} + \tfrac{1}{2}\rho u^2. \tag{1d}$$

The quantities ρ, u, p and γ represent density, velocity, pressure and the ratio of specific heat capacities of the fluid respectively. Equations (1a–d) represent a system of hyperbolic equations for $(\rho, \rho u, e) = (\rho, \rho u, e)(r, t)$, where ρu is the momentum at a general position r along the duct (of cross-sectional area $S(r)$) at time t. The particular example $S(r) = r^N$ represents slab symmetry ($N = 0$), cylindrical symmetry ($N = 1$) or spherical symmetry ($N = 2$). (N.B. The co-ordinate r is given by $r = x$, $\sqrt{(x^2 + y^2)}$ and $\sqrt{(x^2 + y^2 + z^2)}$ in the case of central symmetry with $N = 0$, 1 and 2 respectively, where x, y and z represent Cartesian co-ordinates.)

In the next section we find approximate solutions of equations (1a–d), but first we rewrite them in standard 'conservation form' as

$$\mathbf{w}_t + (\mathbf{F}(\mathbf{w}))_r = \mathbf{f}(\mathbf{w}), \tag{2a}$$

where

$$\mathbf{w} = (\rho, \rho u, e)^{\mathrm{T}}, \qquad \mathbf{F}(\mathbf{w}) = (\rho u, p + \rho u^2, u(e + p))^{\mathrm{T}}, \tag{2b,c}$$

together with (1d), and

$$\mathbf{f}(\mathbf{w}) = -S'(r)/S(r)(\rho u, \rho u^2, u(e + p))^{\mathrm{T}} \tag{2d}$$

is a source term arising from the geometry. The special case $S(r) =$ constant is considered first and the extension to the general case is developed from the special case.

3. APPROXIMATE RIEMANN SOLVER

We consider the approximate solution $\mathbf{w}_j^n \simeq \mathbf{w}(r_j, t_n)$ to consist of a set of piecewise constants and solve approximately the associated Riemann problems at the interface separating adjacent states. An approximate Jacobian needs to be constructed across an interface so that shock capturing is automatic, and this represents an average of the Jacobian matrix evaluated either side of the interface.

Consider firstly equations (2a) with $S(r) \equiv$ constant. The Jacobian matrix of the flux function $\mathbf{F}(\mathbf{w})$ is given by

$$A = \frac{\partial \mathbf{F}}{\partial \mathbf{w}} = \begin{pmatrix} 0 & 1 & 0 \\ \dfrac{\gamma - 3}{2}u^2 & (3 - \gamma)u & \gamma - 1 \\ \dfrac{\gamma - 2}{2}u^3 - \dfrac{ua^2}{\gamma - 1} & \dfrac{3 - 2\gamma}{2}u^2 + \dfrac{a^2}{\gamma - 1} & \gamma u \end{pmatrix}. \tag{3}$$

Consider two adjacent states $\mathbf{w}_L$ and $\mathbf{w}_R$ (left and right) given at either end of the cell (r_L, r_R) and consider also the algebraic problem of finding an approximate Jacobian $\tilde{A} = \tilde{A}(\mathbf{w}_L, \mathbf{w}_R)$ in this cell such that

$$\tilde{A}\Delta\mathbf{w} = \Delta\mathbf{F}, \tag{4}$$

where $\Delta(\cdot) = (\cdot)_R - (\cdot)_L$, $\mathbf{w} = (\rho, \rho u, e)^T$ and $\mathbf{F} = (\rho u, p + \rho u^2, u(e + p))^T$. A solution to this problem for arbitrary jumps $\Delta\mathbf{w}$ can be used to obtain a conservative scheme with good shock-capturing properties. Although the matrix $\tilde{A}$ is not unique, it is possible to determine a matrix which results in an efficient algorithm. This is achieved by writing $\Delta\mathbf{w}$ and $\Delta\mathbf{F}$ in terms of $\Delta\mathbf{u}$, where $\mathbf{u} = (\rho, u, p)^T$, and using identities such as $\Delta(\rho u) = \bar{\rho}\Delta u + \bar{u}\Delta\rho$, $\Delta(\rho u^2) = \overline{u^2}\Delta\rho + 2\bar{\rho}\bar{u}\Delta u$ and $\Delta(up) = \bar{u}\Delta p + \bar{p}\Delta u$, where the overbar denotes the arithmetic mean of left and right states. The matrix $\tilde{A}$ which results is

$$\tilde{A} = \begin{pmatrix} 0 & 1 & 0 \\ \dfrac{\gamma-3}{2}\hat{u}^2 & (3-\gamma)\bar{u} & \gamma - 1 \\ \dfrac{\gamma-2}{2}\bar{u}\hat{u}^2 - \dfrac{\bar{u}\widetilde{a^2}}{\gamma-1} & \dfrac{\widetilde{a^2}}{\gamma-1} + \tfrac{3}{2}\widetilde{u^2} - \gamma\bar{u}^2 & \gamma\bar{u} \end{pmatrix}, \tag{5}$$

where

$$\overline{u^2} = \tfrac{1}{2}(u_L^2 + u_R^2), \qquad \hat{u} = \sqrt{(u_L u_R)}, \qquad \widetilde{u^2} = \tfrac{1}{3}(u_L^2 + u_L u_R + u_R^2), \tag{6a–c}$$

$$\widetilde{a^2} = \gamma\bar{p}/\bar{\rho} \tag{7}$$

$$\bar{u} = \tfrac{1}{2}(u_L + u_R), \qquad \bar{\rho} = \tfrac{1}{2}(\rho_L + \rho_R), \qquad \bar{p} = \tfrac{1}{2}(p_L + p_R), \tag{8a–c}$$

and this matrix satisfies (4).

Now the important quantities that are needed for the scheme are the eigenvalues $\tilde{\lambda}_i$ and eigenvectors $\tilde{\mathbf{e}}_i$ of $\tilde{A}$ and it is a simple matter to show that these are given by

$$\tilde{\lambda}_{1,2,3} = \bar{u} \pm \tilde{a}, \bar{u} \tag{9a–c}$$

$$\tilde{\mathbf{e}}_{1,2} = \left(1, \bar{u} \pm \tilde{a}, \frac{\widetilde{a^2}}{\gamma-1} + \tfrac{1}{2}\overline{u^2} \pm \bar{u}\tilde{a}\right)^T, \qquad \tilde{\mathbf{e}}_3 = \left(1, \bar{u}, \tfrac{1}{2}\overline{u^2} - \frac{(\Delta u)^2}{4(\gamma-1)}\right)^T, \tag{10a–c}$$

where

$$\tilde{a} = [\widetilde{a^2} + \tfrac{1}{4}(\Delta u)^2]^{1/2}. \tag{11}$$

Finally it is necessary to project a general jump $\Delta\mathbf{w}$ on to the eigenvectors $\tilde{\mathbf{e}}_i$ as

$$\Delta\mathbf{w} = \sum_{i=1}^{3} \tilde{\alpha}_i \tilde{\mathbf{e}}_i. \tag{12}$$

By virtue of equation (4) we then have

$$\Delta\mathbf{F} = \sum_{i=1}^{3} \tilde{\lambda}_i \tilde{\alpha}_i \tilde{\mathbf{e}}_i. \tag{13}$$

Solving equation (12) gives

$$\tilde{\alpha}_{1,2} = \frac{\Delta p \pm \bar{\rho}\tilde{a}\Delta u + \frac{1}{4}(\Delta u)^2 \Delta\rho}{2\tilde{a}^2}, \qquad \tilde{\alpha}_3 = \frac{\widetilde{a^2}}{\tilde{a}^2}\Delta\rho - \frac{\Delta p}{\tilde{a}^2}. \tag{14a–c}$$

Thus equations (2a) with $S(r) \equiv$ constant can be approximated by

$$\frac{\mathbf{w}_P^{n+1} - \mathbf{w}_P^n}{\Delta t} + \frac{\Delta \mathbf{F}}{\Delta r} = \mathbf{0}, \tag{15}$$

which can thus be written as

$$\frac{\mathbf{w}_P^{n+1} - \mathbf{w}_P^n}{\Delta t} + \sum_{i=1}^{3} \frac{\tilde{\lambda}_i \tilde{\alpha}_i \tilde{\mathbf{e}}_i}{\Delta r} = \mathbf{0}, \tag{16}$$

where Δr and Δt represent the mesh spacing in the r- and t-directions respectively and the point P may be L or R. Upwind differencing now applied to equation (16) gives the following first-order algorithm for the solution of equations (2a) with $S(r) \equiv$ constant:

$$\text{add} \quad -\frac{\Delta t}{\Delta r}\tilde{\lambda}_i \tilde{\alpha}_i \tilde{\mathbf{e}}_i \text{ to } \mathbf{w}_R \text{ when } \tilde{\lambda}_i > 0 \quad \textit{or} \quad \text{add} \quad -\frac{\Delta t}{\Delta r}\tilde{\lambda}_i \tilde{\alpha}_i \tilde{\mathbf{e}}_i \text{ to } \mathbf{w}_L \text{ when } \tilde{\lambda}_i < 0. \tag{17}$$

The only quantities required for the algorithm are given by equations (6a) and (11), so that only one square root is taken in each computational cell. The first-order algorithm can be extended to second-order accuracy using flux limiters[6] and can be modified to be entropy-satisfying by employing the scalar algorithm in Reference 7. For a discussion on overcoming the problem of flows near a vacuum the reader is referred to the work of Einfeldt.[8]

Finally, in the case of a duct of variable cross-section or for cylindrically or spherically symmetric flows, there is a source term present, $\mathbf{f} = -S'(r)/S(r)\ (\rho u, \rho u^2, u(e+p))^T$. Upwinding the source term as described in Reference 4 enables equations (2a) to be solved approximately using appropriately modified wave strengths $\tilde{\alpha}_i$.

4. TEST PROBLEMS AND NUMERICAL RESULTS

We describe five test problems and give the numerical results obtained for each using the scheme of Section 3.

Problem 1

This is the well-known shock tube problem of Sod[9] for the Euler equations in slab symmetry $S(r) \equiv 1$ with $\gamma = 1{\cdot}4$ and initial data

$$\rho, u, p = \begin{cases} 1, 0, 1, & x < \frac{1}{2}, \\ 0{\cdot}125, 0, 0{\cdot}1, & x > \frac{1}{2}. \end{cases}$$

The main features of the exact solution are a shock moving to the right, followed by a contact discontinuity also moving to the right, but more slowly, and an expansion fan moving to the left.

Figure 1 shows the approximate and exact solutions for ρ, u, p and e at $t = 0{\cdot}144$ s using 100 mesh points. It is clear that the approximate solution models the exact solution.

Problem 2

This problem is usually described as 'two interacting blast waves' and is a shock tube problem for the Euler equations in slab symmetry with $\gamma = 1{\cdot}4$ and initial data

$$\rho,\ u,\ p = \begin{cases} 1, 0, 1000, & 0 < x < 0{\cdot}1, \\ 1, 0{\cdot}01, 0{\cdot}1, & 0{\cdot}1 < x < 0{\cdot}9, \\ 1, 0, 100, & 0{\cdot}9 < x < 1. \end{cases}$$

The walls of the tube at $x = 0$ and 1 are assumed to be perfectly reflecting. Two strong blast waves develop and collide, producing a complex flow. A detailed description of the time evolution of the flow can be found in Reference 10.

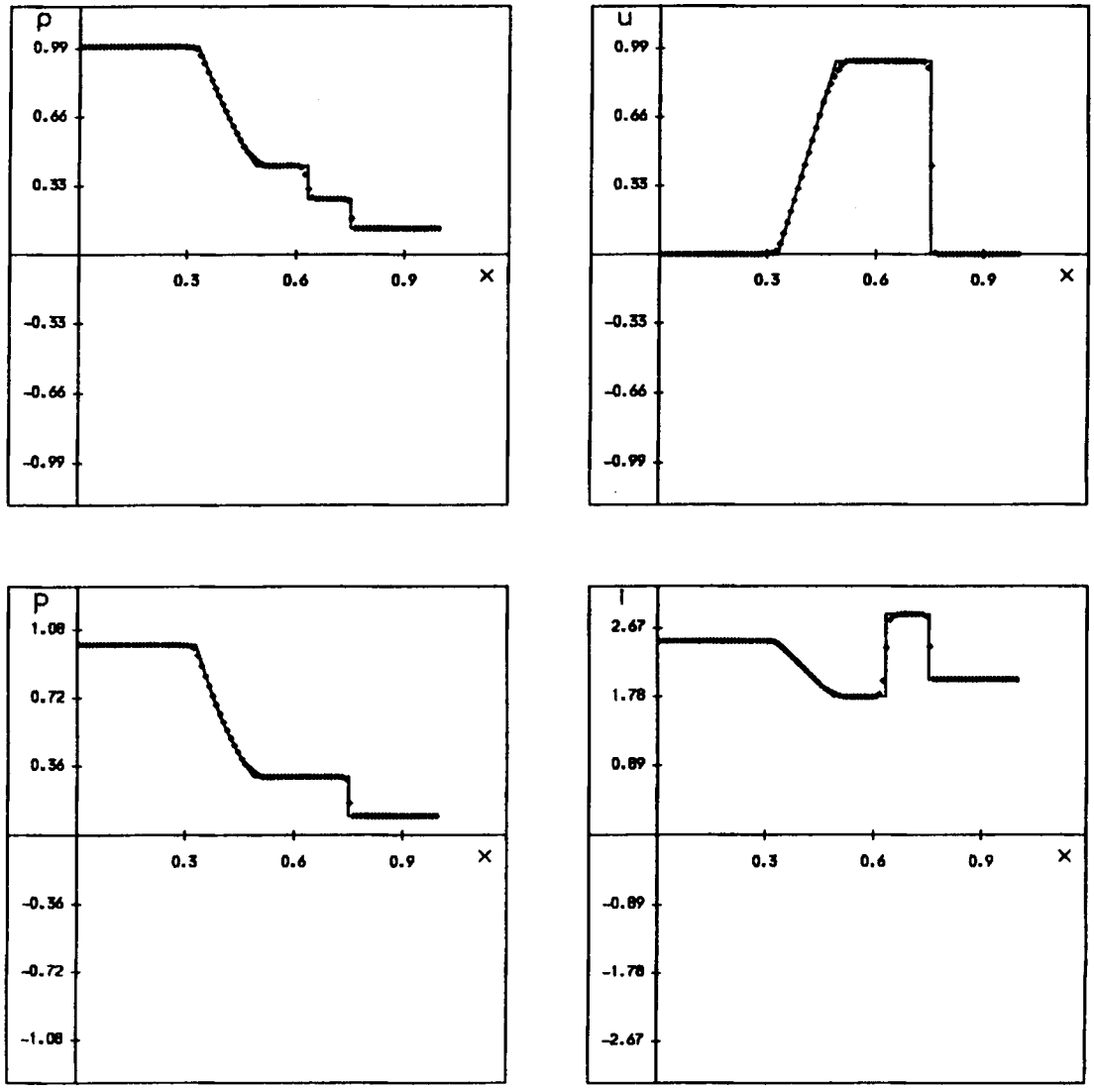

Figure 1. Approximate solution for Problem1

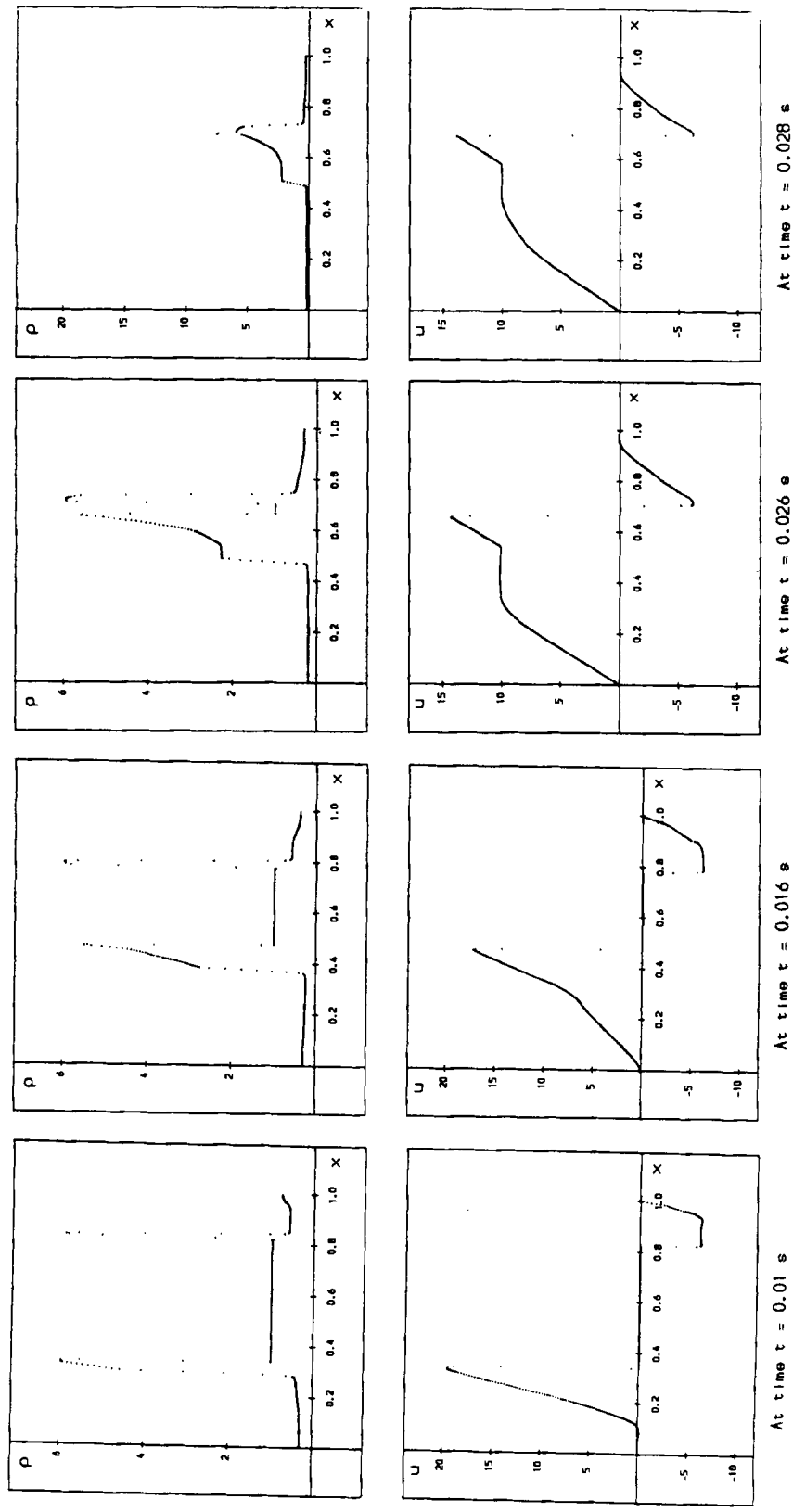

Figure 2. Approximate solution for Problem 2

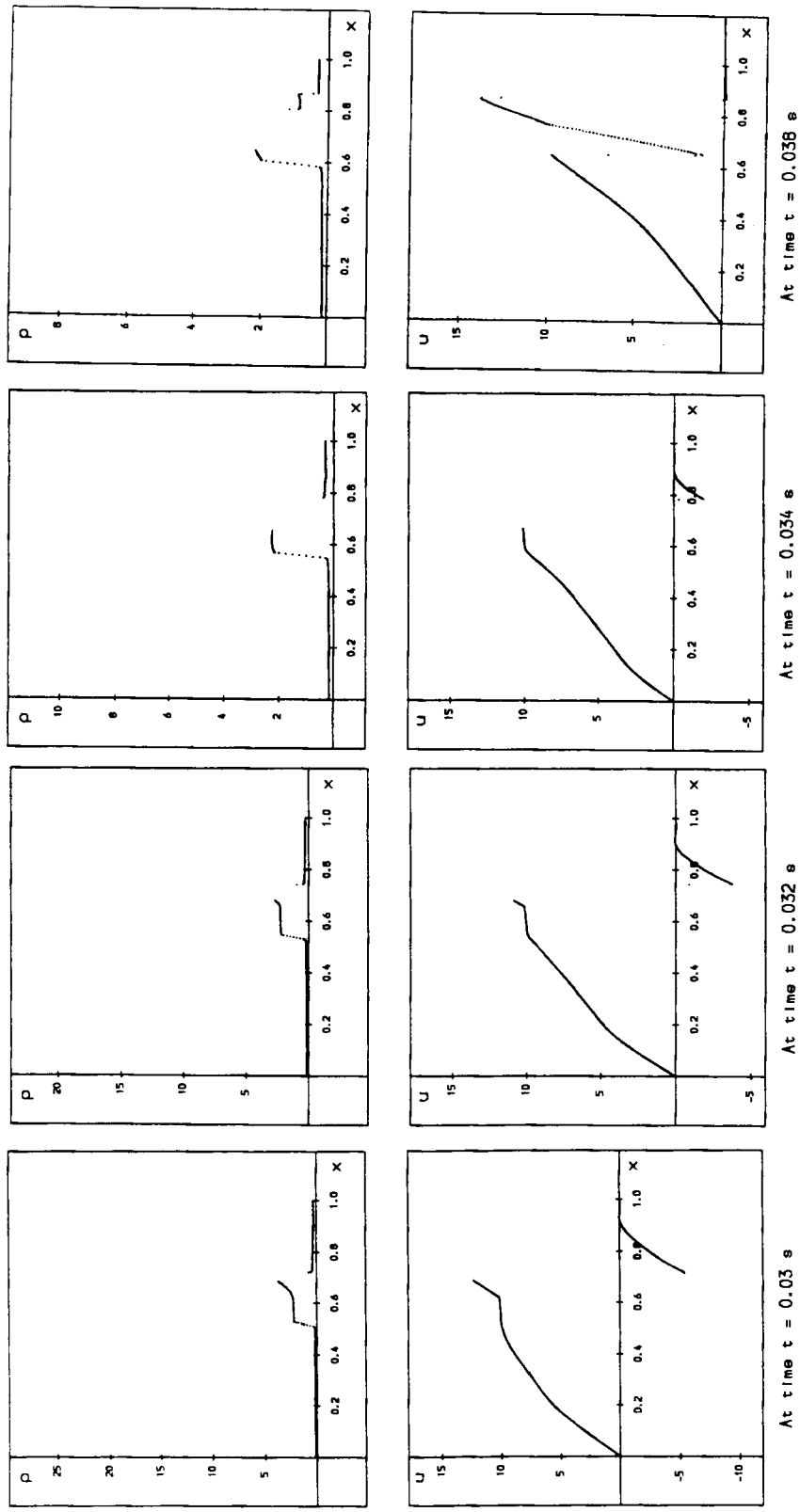

Figure 3. Approximate solution for Problem 2

SOLUTION OF THE EULER EQUATIONS WITH SLAB SYMMETRY - Shock Reflection

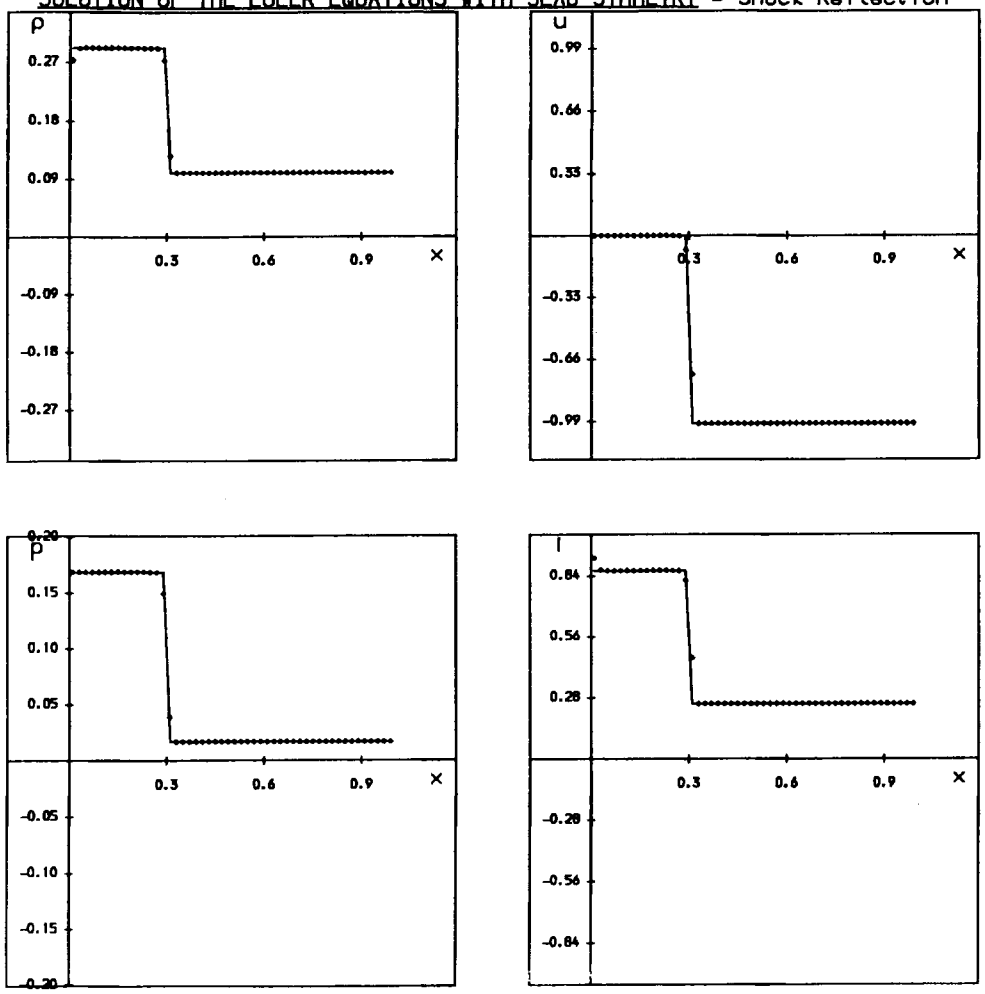

at time t = 0.575

KEY

ρ - Density
u - Velocity
p - Pressure
I - Internal energy

—— Exact solution
◇◇◇◇◇ Approximate solution

PARAMETERS

equation of state
for an ideal gas
50 Mesh points
89 Time steps
Δx = 0.02
Δt = 0.0065
Pressure ratio = 10
"Superbee" limiter used

INITIAL CONDITIONS

ρ = 0.100
u = -1.000
p = 0.017
(I = 0.254)

0

Reflected Boundary Conditions
at x = 0

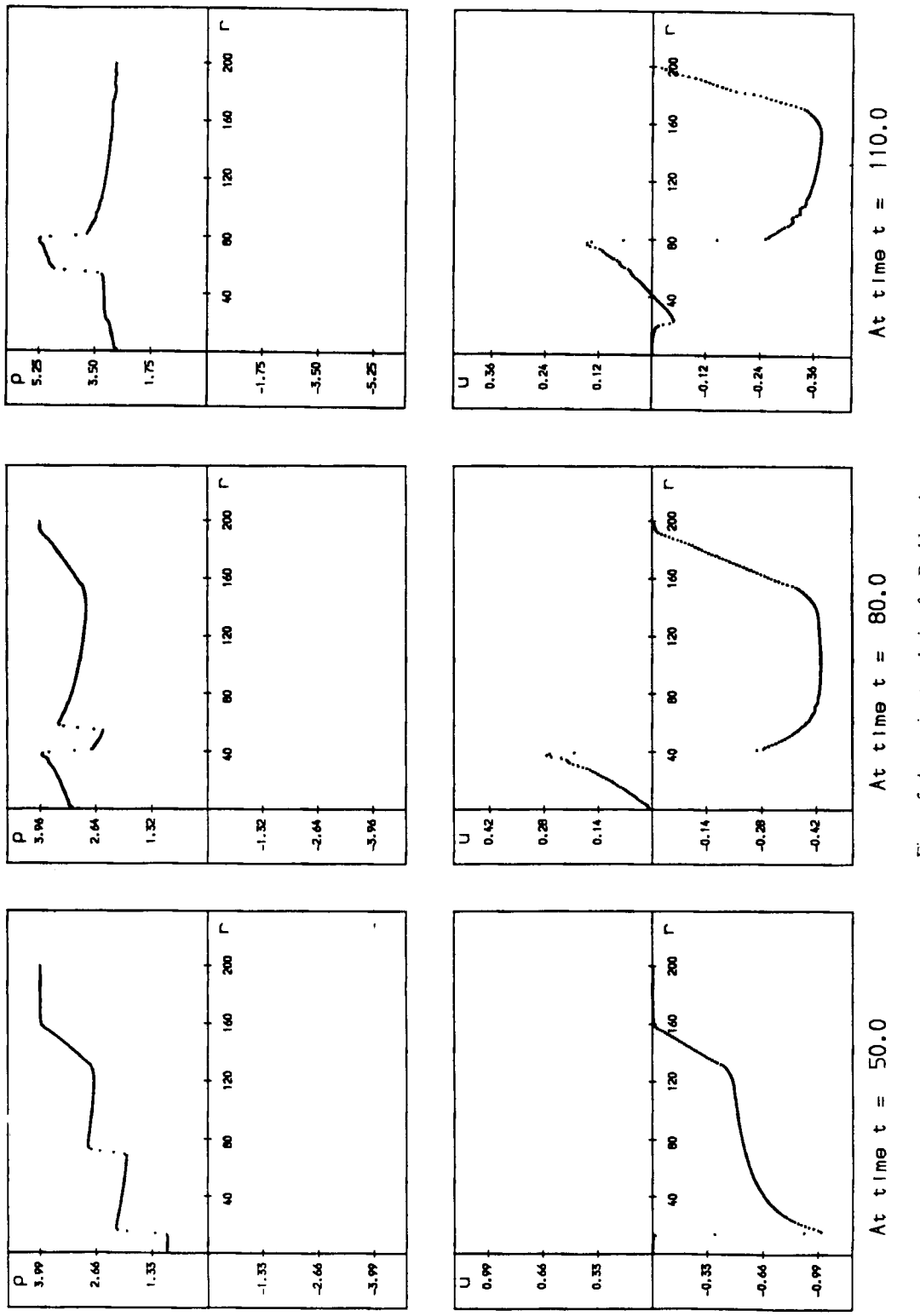

Figure 5. Approximate solution for Problem 4

Figures 2 and 3 show the approximate solution for ρ and u at $t = 0{\cdot}01$, $0{\cdot}016$, $0{\cdot}026$, $0{\cdot}028$, $0{\cdot}03$, $0{\cdot}032$, $0{\cdot}034$ and $0{\cdot}038$ s using 400 mesh points. The results are comparable with those given in Reference 10 using a more complicated Riemann solver.

Problem 3

This problem is concerned with shock reflection for the Euler equations in slab symmetry with $\gamma = \frac{5}{3}$ and initial data ρ, u, $p = 1$, -1, $0{\cdot}017$ in the interval $0 \leqslant x \leqslant 1$. This represents gas of a constant density and pressure moving towards $x = 0$ which is a rigid wall. The exact solution describes shock reflection from the wall and the reflected shock, of strength 10, propagates towards $x = 1$ with constant speed.

Figure 4 shows the approximate and exact solutions when the shock has moved a distance of $0{\cdot}3$. It is clear that the approximate solution models the exact solution.

Problem 4

This problem is concerned with a converging cylindrical shock and we consider a region $0 \leqslant r \leqslant 200$ for the cylindrically symmetric Euler equations with $S(r) = r$ and $\gamma = 1{\cdot}4$. Initially a cylindrical diaphragm of radius $r = 100$ separates two uniform regions of gas at rest. The initial conditions are $\rho = 4$, $p = 4$ in the outer region and $\rho = 1$, $p = 1$ in the inner region. When the diaphragm is removed at $t = 0$, a converging shock wave, followed by a converging contact discontinuity, moves towards the axis, $r = 0$, and a diverging rarefaction wave moves outwards. The shock accelerates as it approaches the axis of symmetry, is reflected from the axis and interacts with the contact discontinuity (still converging), which results in a transmitted shock, a converging contact discontinuity and a weak converging reflected shock.

Figure 5 shows the approximate solution at times $t = 50$, 80 and 110 with 200 mesh points. The results are comparable with results produced using a more complex algorithm.[11]

Problem 5

The final test problem is concerned with a converging and a diverging cylindrical shock in the region $0 \leqslant r \leqslant 200$ for the cylindrically symmetric Euler equations, again with $\gamma = 1{\cdot}4$. Initially two cylindrical diaphragms of radii $r = 50$ and 150 separate three uniform regions of gas at rest. The initial conditions are $\rho = 4$, $p = 4$ in the inner and outer regions and $\rho = 1$, $p = 1$ in the middle region. When the diaphragms are removed at $t = 0$, a converging shock wave, followed by a converging contact discontinuity, moves towards the axis, $r = 0$, and a diverging shock wave, followed by a diverging contact discontinuity, moves away from the axis. The shocks subsequently interact, resulting in a diverging shock wave weakening in strength, together with a converging shock wave increasing in strength. Each of these shocks then interacts with the corresponding contact discontinuity as in Problem 4, resulting in a transmitted shock, a weak reflected shock and a contact discontinuity for each interaction.

Figure 6 shows the approximate solution at times $t = 30$, 40 and 60 using 200 mesh points. We observe the development of the shocks and contact discontinuities, the interaction of shocks and the subsequent interaction of each shock with a contact discontinuity, resulting in transmitted and reflected shocks and contact discontinuities.

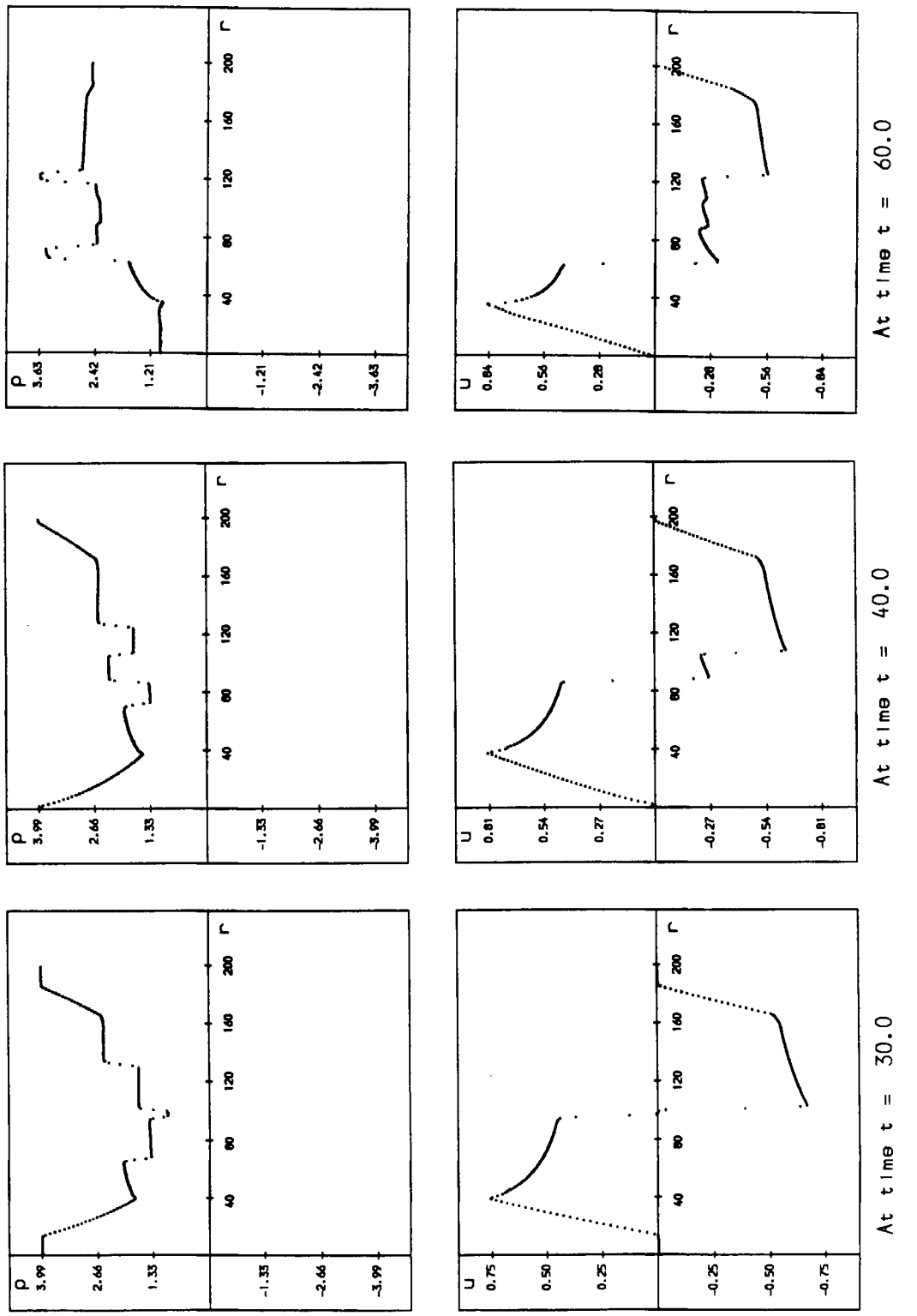

Figure 6. Approximate solution for Problem 5

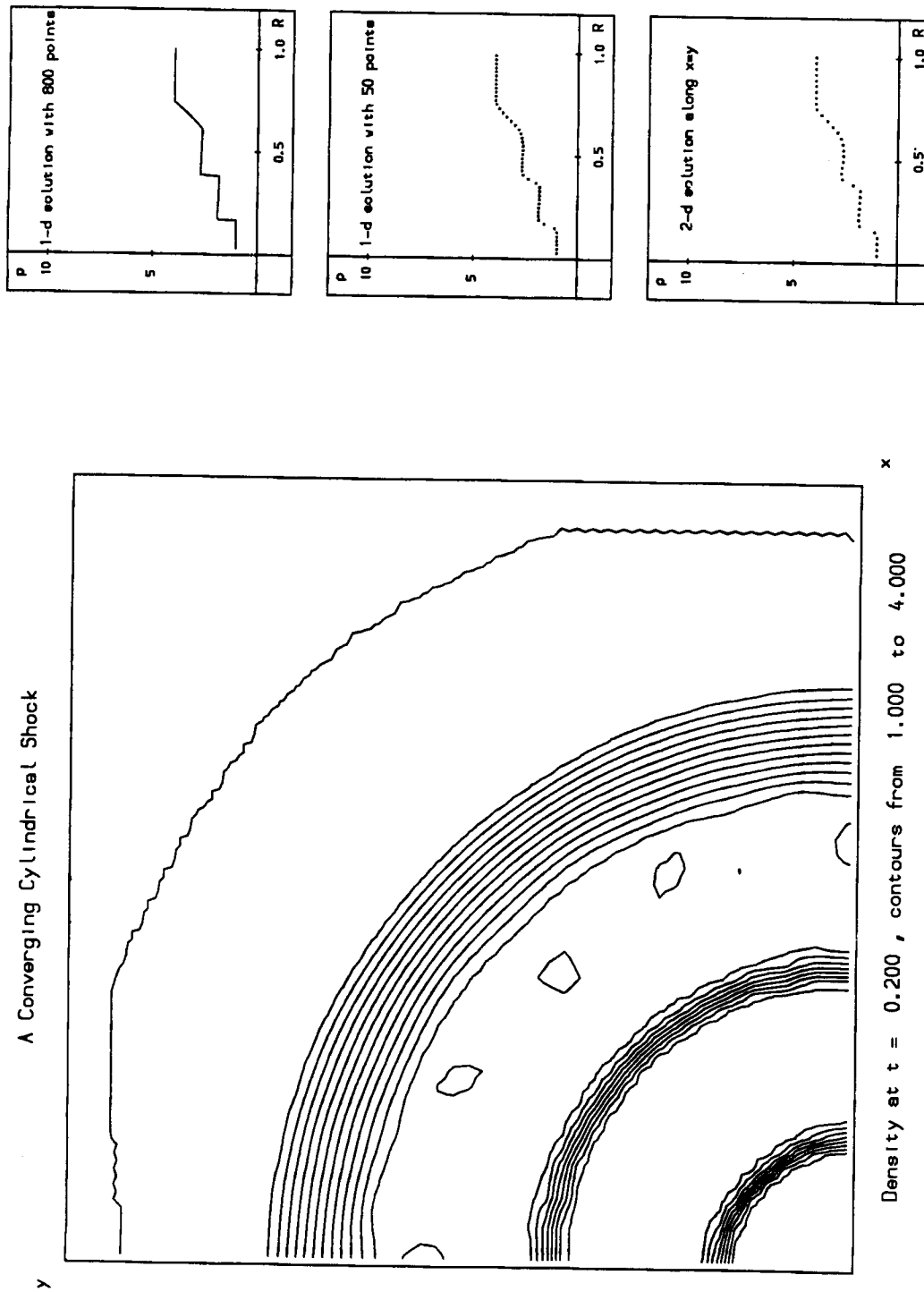

Figure 7. Comparison of two-dimensional solution with 'one-dimensional' solution

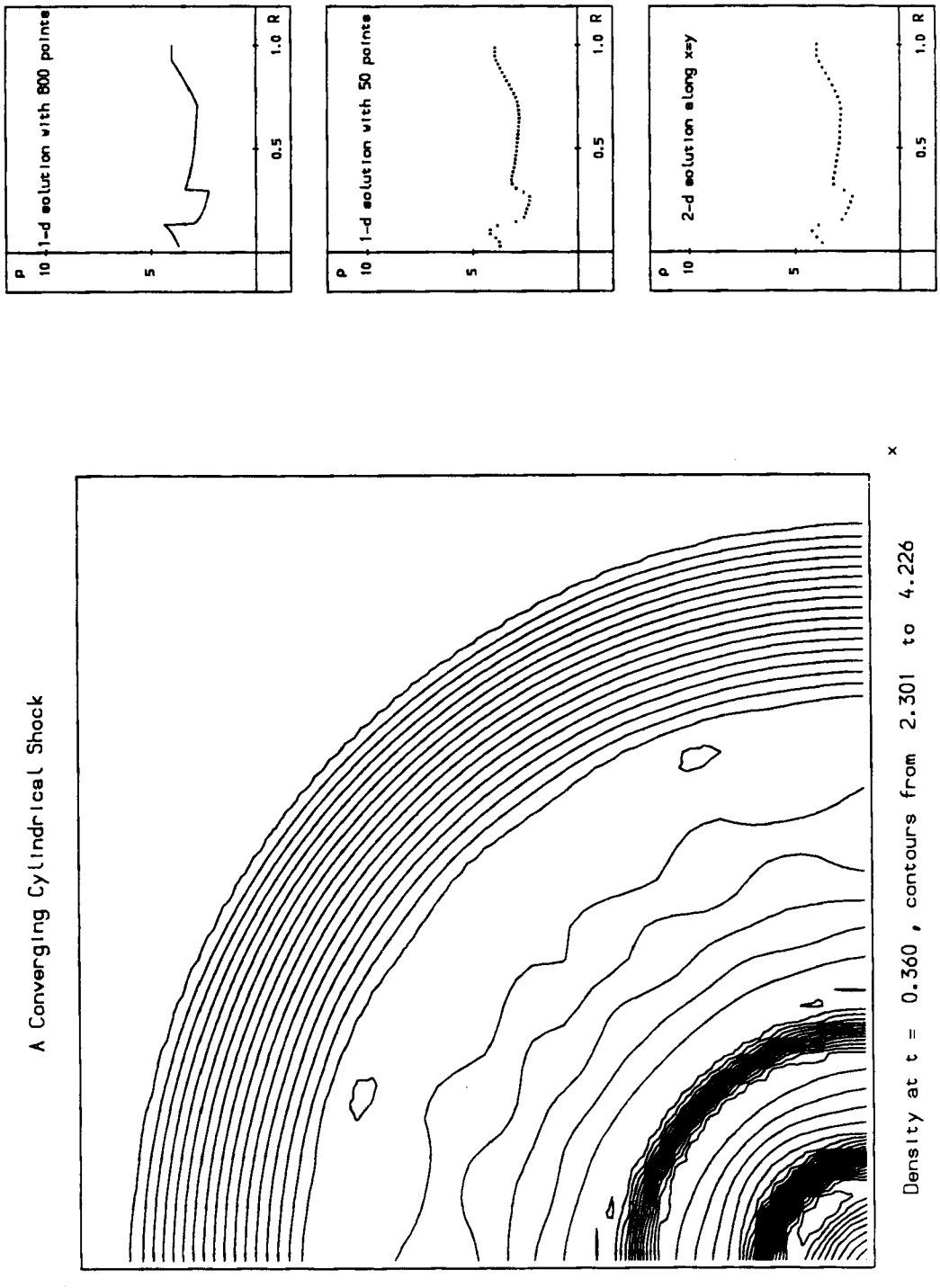

Figure 8. Comparison of two-dimensional solution with 'one-dimensional' solution

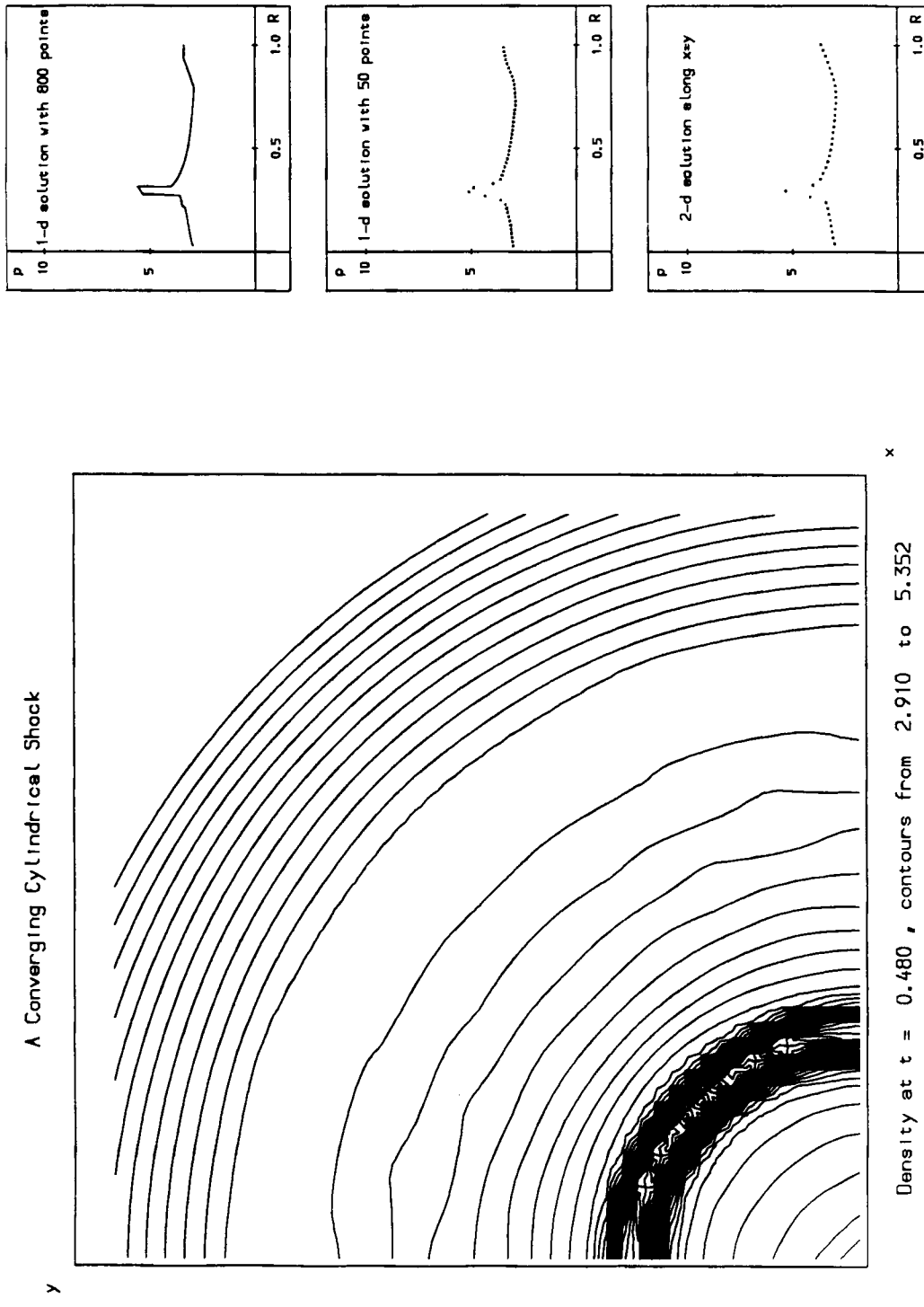

Figure 9. Comparison of two-dimensional solution with 'one-dimensional' solution

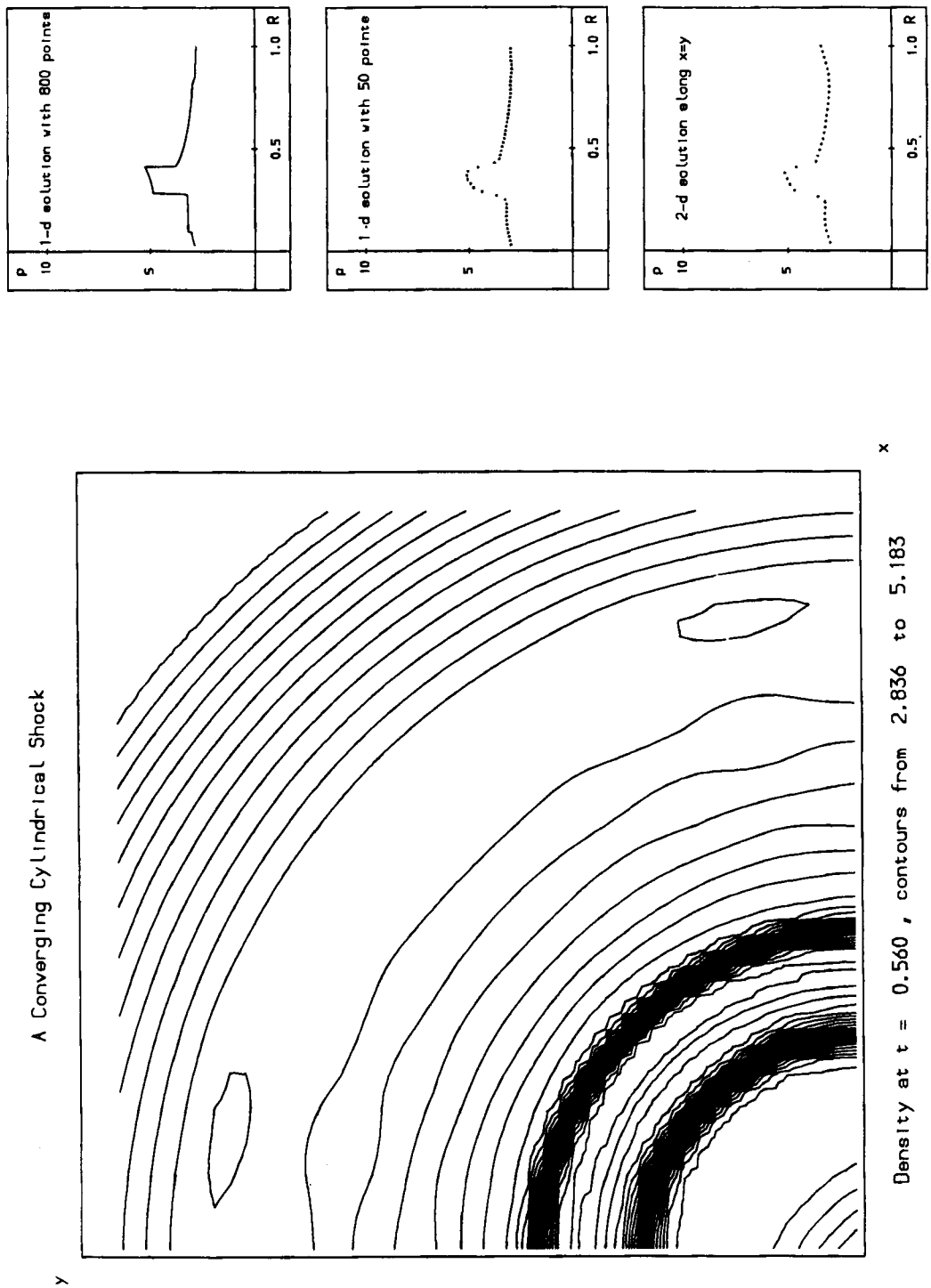

Figure 10. Comparison of two-dimensional solution with 'one-dimensional' solution

Finally, Figures 7–10 show the density results for a two-dimensional, cylindrically symmetric shock tube problem solved in two dimensions with a 50 × 50 mesh and in 'one dimension' using 50 and 800 mesh points. Again it is clear that the approximate solutions in one and two dimensions are comparable and the convergence to a physically acceptable solution is obtained.

A comparison of the computational expense has been made using an Amdahl V7 and the results are as follows. Using Roe's 'square root' averaging and the 'Superbee' limiter[6] with 100 mesh points takes 0·0142 CPU seconds to compute one time step, whereas the scheme presented here using arithmetic averages takes 0·0121 CPU seconds to compute one time step.

5. CONCLUSIONS

We have presented an efficient shock-capturing algorithm for the Euler equations utilizing the arithmetic mean for the averages of the flow variables in computational cells. The main features of this scheme are that (i) it can be used for slab, cylindrically or spherically symmetric problems with confidence and (ii) it can be used as a comparison with results from two-dimensional schemes by choosing a large number of mesh points for accuracy and not be expensive on computing.

REFERENCES

1. P. L. Roe, 'Approximate Riemann solvers, parameter vectors and difference schemes', *J. Comput. Phys.*, **43**, 357–372 (1981).
2. S. Osher, 'Riemann solvers, the entropy condition and difference approximations', *SIAM J. Numer. Anal.*, **21**, 217–235 (1984).
3. M. Brio and C. C. Wu, 'An upwind differencing scheme for the equations of ideal magnetohydrodynamics', *J. Comput. Phys.*, **75**, 400–422 (1988).
4. P. Glaister, 'An efficient numerical scheme for the shallow water equations', *Comput. Math.*, **49**(3/4), in press.
5. E. Dick, 'A flux-difference splitting method for steady Euler equations', *J. Comput. Phys.*, **76**, 19–32 (1988).
6. P. K. Sweby, 'High resolution schemes using flux limiters for hyperbolic conservation laws', *SIAM J. Numer. Anal.*, **21**, 995–1011 (1984).
7. P. K. Sweby and M. J. Baines, 'On the convergence of Roe's scheme for the general non-linear scalar wave equation', *J. Comput. Phys.*, **56**, 135–148 (1984).
8. B. Einfeldt, 'On Godunov type methods near low densities', *Cranfield Institute of Technology Rep. 8810*, 1988.
9. G. A. Sod, 'A survey of several finite difference methods for systems of nonlinear hyperbolic conservation laws', *J. Comput. Phys.*, **27**, 1–31 (1978).
10. P. R. Woodward and P. Colella, "The numerical simulation of two-dimensional fluid flow with strong shocks', *J. Comput. Phys.*, **54**, 115–173 (1984).
11. M. Ben-Artzi and J. Falcovitz, 'A second order Godunov-type scheme for compressible fluid dynamics', *J. Comput. Phys.*, **55**, 1–32 (1984).